

## Supporting information

### Electroactive and degradable supramolecular microgels

Helin Li,<sup>a,b</sup> Olga Mergel,<sup>c</sup> Puja Jain,<sup>b</sup> Xin Li,<sup>a,b</sup> Huan Peng,<sup>a,b</sup> Khosrow Rahimi,<sup>b</sup> Smriti Singh,<sup>b</sup> Felix Plamper,<sup>\*c,d</sup> and Andrij Pich<sup>\*a,b</sup>

#### Colloidal stability of microgels

**Characterization methods.** The colloidal stability of microgels dispersions was measured by separation analyzer LUMiFuge 114 (LUM GmbH, Germany).

Sedimentation measurements were carried out in polycarbonate cells at acceleration velocities of 4000 rpm at 25°C. To measure the sedimentation velocity of microgels in the corresponding solvent mixtures, the microgels in PBS buffers were studied.

**Results and discussion.** The colloidal stability behaviors of microgels were evaluated by LUMiFuge at pH 3, 7, and 10. Fig. S1 indicates that the sedimentation velocities of microgels were affected by the chemical structure and change of pH of the medium. These sedimentation velocities can be obtained through analyzing the slope of sedimentation curves.

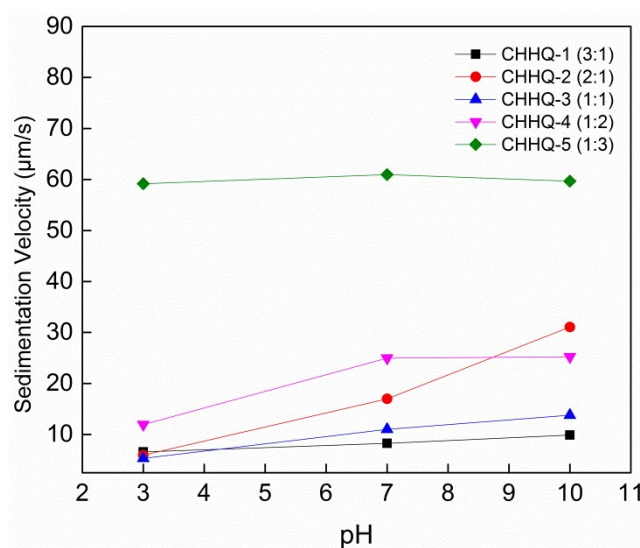


**Fig. S1** Sedimentation velocities of microgels at pH 3, 7 and 10.

The CHHQ-5 has probably the highest tendency to aggregate and therefore the lowest colloidal stability, being reflected in the exceptionally high sedimentation velocity. The microgels sedimented slower in pH 3 than in pH 7 and 10, and that can be explained by the swelling and that there are no strong indications for aggregation, except for CHHQ-5.

### Electrochemical addressability of microgels at Pt electrode

As seen from the cyclic voltammogram, oxygen evolution at high potentials due to water decomposition can lead to an acidification of the electrolyte, which is not completely compensated by the capacity of the buffer (seen in the decrease of pH upon bulk switching, see Main Part). Further, the CV is enriched in features compared to the CV obtained at glassy carbon electrodes (see Main Part), probably due to a joint signature of adsorption phenomena, water decomposition and electrochemical microgel switching.

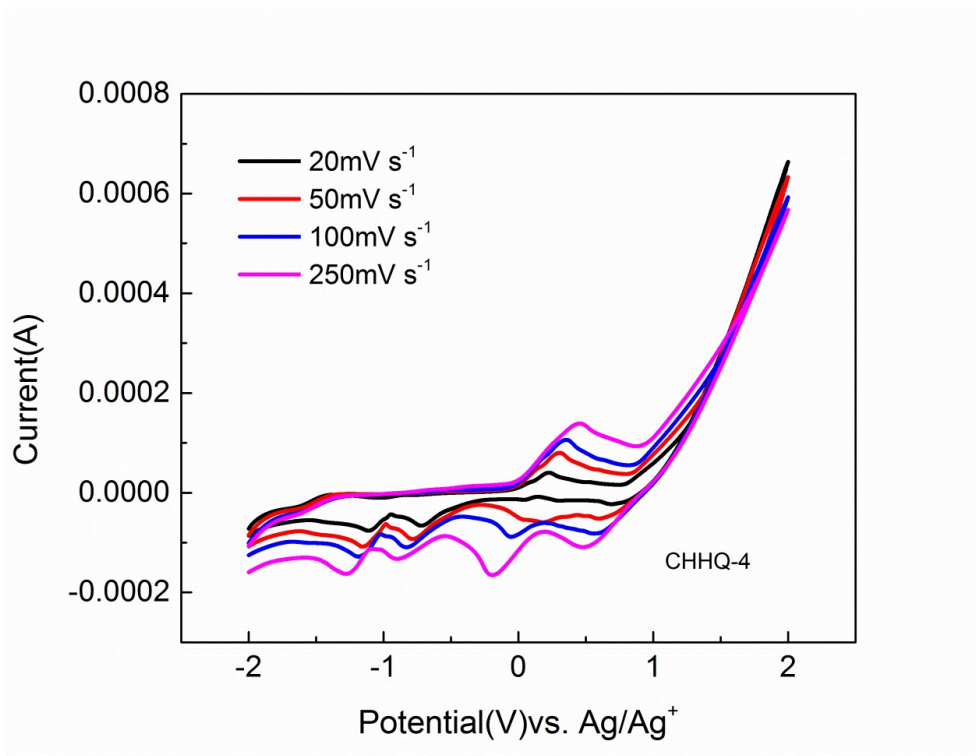


**Fig. S2** Cyclic voltammogram of the microgels (CHHQ-4) in 0.05 mol/L phosphate buffer (pH = 7.3) at different scan rates. Reference electrode is Ag/AgCl and the working electrode is platinum.

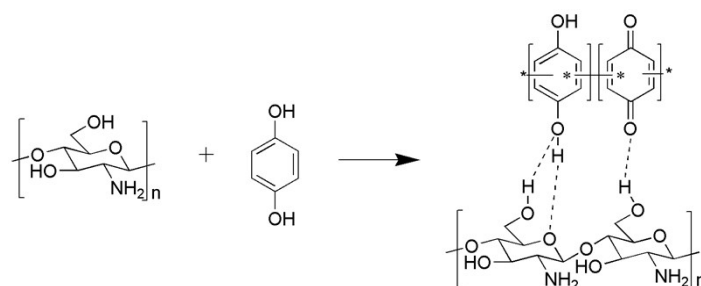
## Chemical Composition of Microgels

| Name of sample | Molar ratio<br>(chitosan/hydroquinone) | Intensity ratio<br>(1077/1204) |
|----------------|--|--------------------------------|
| CHHQ-1         | 0.18                                   | 0.34                           |
| CHHQ-2         | 0.27                                   | 0.50                           |
| CHHQ-3         | 0.55                                   | 1.22                           |
| CHHQ-4         | 1.092                                  | 2.34                           |
| CHHQ-5         | 1.64                                   | 3.36                           |

**Table S1** Ratios of chitosan and poly(hydroquinone) synthesized in microgels.

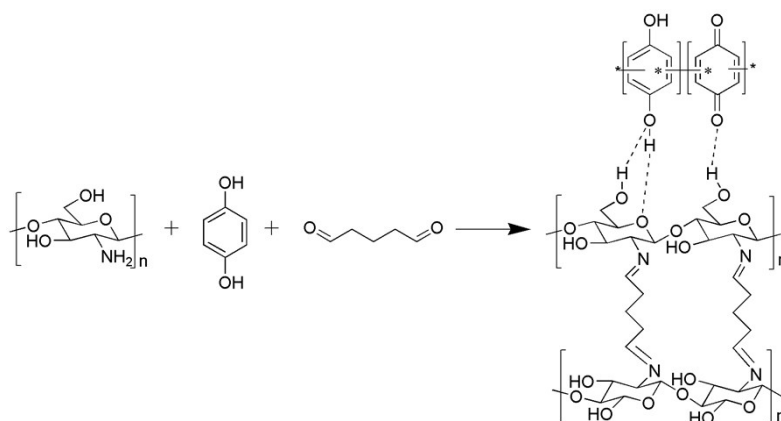
### The synthesis of microgels

**The synthesis of CHHQ microgels.** As shown in Scheme S1, a series of CHHQ microgels were prepared by oxidative polymerization. The microgels were crosslinked by hydrogen bond between chitosan and hydroquinone.



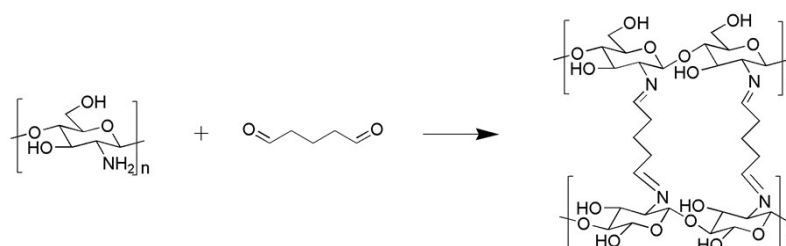
**Scheme S1** Schematic representation of synthesis of CHHQ (chitosan-hydroquinone) microgels.

**The synthesis of CHHQGA microgels.** Scheme S2 illustrated the reaction of synthesis of CHHQGA (chitosan-hydroquinone-glutaraldehyde) microgels. Based on the CHHQ microgel synthesis in which only physical crosslinker formed, the CHHQGA microgels were crosslinked by the physical and chemical crosslinkers during the microgel synthesis. The chemical crosslinkers formed between the amino groups of chitosan and the aldehyde of glutaraldehyde.



**Scheme S2.** Schematic representation of synthesis of CHHQA microgels.

**The synthesis of CHGA microgels.** The reaction of the synthesis of CHGA (chitosan-glutaraldehyde) microgels was shown in Scheme S3. The microgels were only formed by chemical crosslinker. The aldehyde of glutaraldehyde can react with amino groups of the chitosan, and the microgels thus obtained.



**Scheme S3.** Schematic representation of synthesis of CHGA (chitosan-glutaraldehyde) microgels.

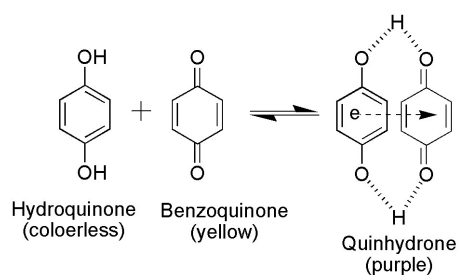
#### Chemical Composition of Microgels.

| Sample name    | Mass ratio of chitosan to hydroquinone | Chitosan, (g) | Hydroquinone, (g) | Glutaraldehyde, (g) |
|----------------|--|---------------|-------------------|---------------------|
| Type 1 CHHQ-4  | 1:2                                    | 0.012         | 0.024             | -                   |
| Type 2 CHHQA-4 | 1:2                                    | 0.012         | 0.024             | 0.01192             |
| Type 3 CHGA    | -                                      | 0.012         | -                 | 0.01192             |

**Table S2** Chitosan, hydroquinone and glutaraldehyde amounts used for microgel synthesis to study the supramolecular assembly within the microgels.

### The complexation of hydroquinone and benzoquinone.

As shown in Scheme S4, the hydroquinone and benzoquinone could be complexed into quinhydrone, which would induce the color of microgel dispersion changed in different buffers.



**Scheme S4.** The schematic representation of complexation of hydroquinone and benzoquinone.

### Degradation of microgels.

The degradation behaviors of microgels were monitored by lysozyme at different concentrations and bovine serum albumin (BSA). The results indicate that the microgels could be degraded by lysozyme.

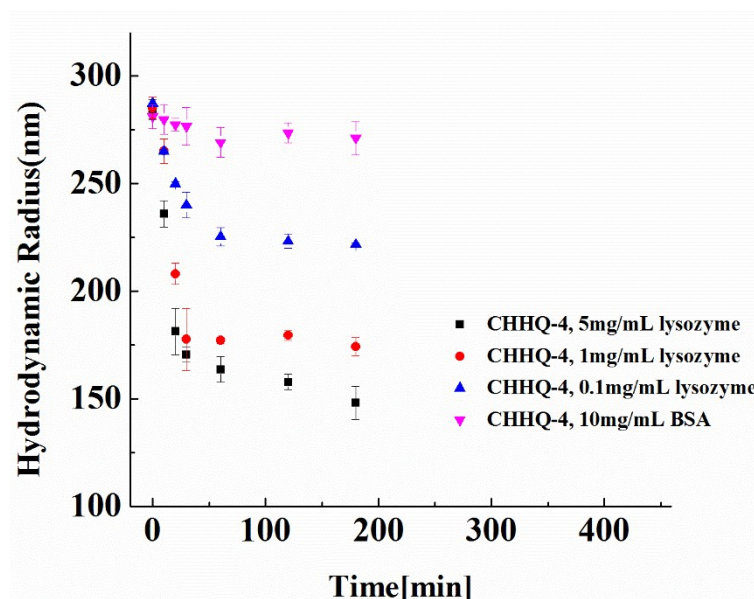


**Fig. S2** Degradation of the microgels (CHHQ-4) in pH 6 buffer in the presence of lysozyme and BSA.